Ahmed Mohammedi[1], Djamila Rekioua [1,*] Nabil Mezzai[1],

J. Electrical Systems 9-2 (2013): 212-222

Regular paper

Experimental Study of a PV Water Pumping System

Journal of Electrical Systems

In this paper, we present different performances of a photovoltaic (PV) water pumping system. A prototype of experimental bench in installed in the laboratory of industrial technology and information (LTII). We present a model to characterize the motor-pump subsystem used in PV pumping installations. The model expresses the water flow output (Q) directly as a function of the electrical power input (P) to the motor-pump, for different total heads. The obtained experimental results illustrated by curves are represented and analyzed.

Keywords: Photovoltaic, water pumping system, centrifugal pump, MPPT

1. Introduction

The photovoltaic pumping has become one of the most promising fields in photovoltaic applications. To achieve the operation's most reliable and most economical; more attention is paid to their design and their optimal use. Depending upon the intended application, the pumping system can be selected from surface, submersible or floating pumps types [1]. Pumps can be classified according to their operating mode. Mainly there are centrifugal and positive displacement pumps [1]. In the centrifugal pump, the rotation of an impeller forces water into the pipe. The water velocity and pressure depend on the available mechanical power at the rotating impeller and the total head. The displacement pump uses a piston or a screw to control the water flow. As compared to the centrifugal pump, the positive displacement pump presents a better efficiency under low power conditions. The water pumps may be driven by direct current (DC) or alternatif current (AC) motors. The earlier PV pumping systems were principally based on DC motors [2]. The DC motors present the drawback of maintenance expenses due to frequent brushes replacements [5]. Brushless permanent magnet DC motors have been introduced in some systems [3]. Recent developments in induction motor technology, made this option attractive among the AC motors based pumping setups [4]. The induction motor is more robust, requires much less maintenance and is available at lower costs than DC motors [3].

Depending upon the intended application, the pumping system can be selected from surface, submersible or floating pumps types [1]. Submersible pumps remain underwater, surface pumps are mounted at water level at the vicinity of the well or, in the case of a floating pump, on top of the water. Pumps can be classified according to their operating mode. Mainly there are centrifugal and positive displacement pumps [1]. As compared to the centrifugal pump, the positive displacement pump presents a better efficiency under low power conditions.

In this paper, we present different performances of a PV water pumping system. A prototype of experimental bench is installed in our laboratory (LTII). The obtained results illustrated by curves are represented and analyzed.

2. Proposed Studied System

* Corresponding author: D. Rekioua, LTII Laboratory, University of Bejaia, E-mail: dja_rekioua@yahoo.fr
[1] L.T.I.I Laboratory, University of Bejaia 06000, Algeria

The experimental water pumping system (Fig.1) comprises PV module feeding a DC motor via DC-DC boost converter with maximum power point tracker (MPPT).

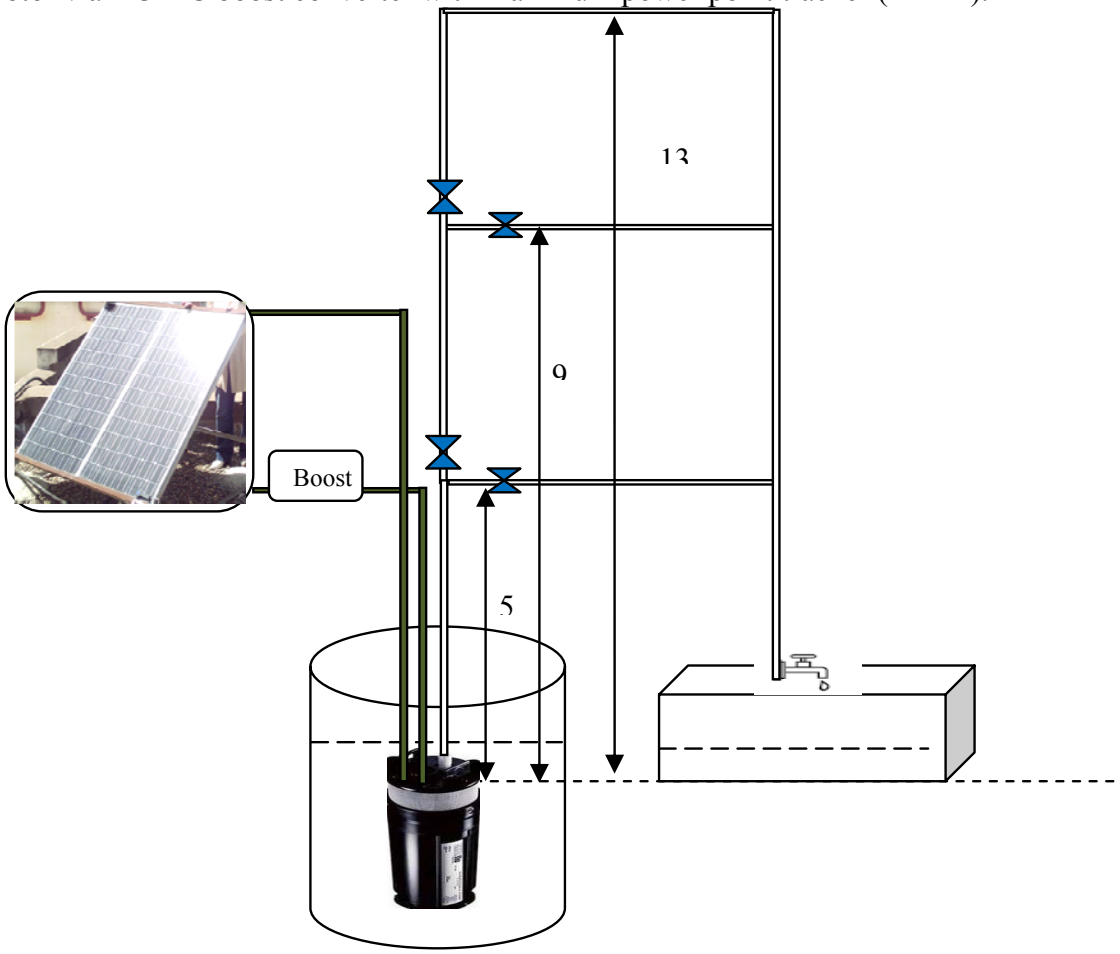

Fig.1. Experimental water pumping system

2.1. PV arrays Modeling

In literature, there are several mathematical models that describe the operation and behavior of the photovoltaic generator [4]. These models differ in the calculation procedure, accuracy and the number of parameters involved in the calculation of the current-voltage characteristic.

2.1.1. First PV model

The model is called one diode and the equivalent circuit (Fig.2) consists of a single diode for the cell polarization phenomena and two resistors (series and shunt) for the losses.

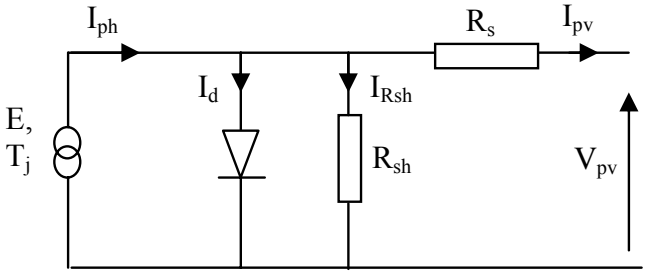

Fig.2. Simplified equivalent circuit of solar cell

$I_{pv}(V_{pv})$ characteristic of this model is given by the following equation [1]:

$$I_{pv} = I_{ph} - I_d - I_{Rsh} \tag{1}$$

$$I_{pv} = I_{ph} - I_0 \left[e^{q \frac{(V_{pv} + I_{pv} . R_s)}{AkT_j}} - 1 \right] - \frac{V_{pv}}{R_{sh}} \tag{2}$$

The photocurrent, Iph, is directly dependent upon both insolation and panel temperature, and may be written in the following form:

$$I_{ph} = P_1 . E . \left[1 + P_2 . (E - E_{ref}) + P_3 . (T_j - T_{ref}) \right] \tag{3}$$

Where*: E* insolation in the panel plane (W/m²); E_{ref} corresponds to the reference insolation of 1000 W/m² and T_{jref} to the reference panel temperature of 25°C. P_1, P_2 and P_3 are constant parameters.
The polarization current I_d of junction PN, is given by the expression:

$$I_d = I_0 . [\exp(\frac{q.(V_{pv} + R_s . I_{pv})}{A.n_s.k.T_j}) - 1] \tag{4}$$

With: I_0 (A) saturation current, q the elementary charge (ev), k Botzman's constant, A ideality factor of the junction, *Tj* : junction temperature of the panels (°K) and R_s, R_{sh} (Ω) resistors (series and shunt).

2.1.2. Second PV Model

The PV array equivalent circuit current I_{pv} can be expressed as a function of the PV array voltage V_{pv}:

$$I_{pv} = I_{sc} \left\{ 1 - C_1 \left[\exp C_2 V_{pv}^m - 1 \right] \right\} \tag{5}$$

Where the coefficients C_1, C_2 and m are defined as:

$$C_1 = 0.01175 \tag{6}$$

$$C_2 = \frac{C_4}{V_{oc}^m} \tag{7}$$

$$C_3 = \ln \left[\frac{I_{sc} (1 + C_1) - I_{mpp}}{C_1 I_{sc}} \right] \tag{8}$$

$$C_4 = \ln \left[\frac{1 + C_1}{C_1} \right] \tag{9}$$

$$m = \frac{\ln\left[\frac{C_3}{C_4}\right]}{\ln\left[\frac{V_{mpp}}{V_{oc}}\right]} \quad (10)$$

With: V_{mpp} voltage at maximum power point; V_{oc} open circuit voltage; I_{mpp} current at maximum power point; I_{sc} short circuit current.

Equation 5 is only applicable at one particular insolation level E, and cell temperature, T_j, at standard test conditions (STC) (E=1000 W/m^2, T_j=25 °C). When insolation and temperature vary, the parameters change according to the following equations:

$$\Delta T_j = T_j - T_{jref} \quad (11)$$

$$\Delta I_{pv} = \alpha_{sc}\left(\frac{E}{E_{ref}}\right)\Delta T_j + \left(\frac{E}{E_{ref}} - 1\right) I_{sc,ref} \quad (12)$$

$$\Delta V_{pv} = -\beta_{oc}\Delta T_j - R_s \Delta I_{pv} \quad (13)$$

Where: α_{sc} current temperature coefficient; βoc voltage temperature coefficient

The new values of the photovoltaic voltage and the current are given by:

$$V_{pv,new} = V_{pv} + \Delta V_{pv} \quad (14)$$

$$I_{pv,new} = I_{pv} + \Delta I_{pv} \quad (15)$$

2.1.3. Third PV model

In the two diodes model, diodes are present for the PN junction polarization phenomena. These diodes represent the recombination of the minority carriers, which are located both at the surface of the material and within the volume of the material (Fig.3).

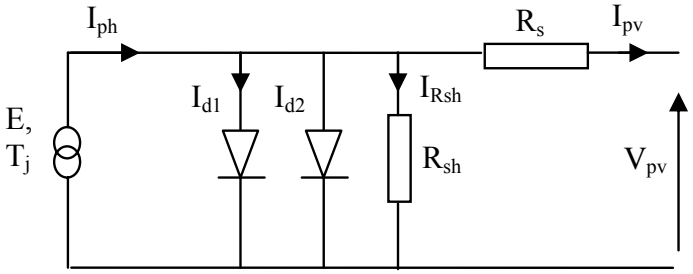

Fig.3. Equivalent circuit for two diode model

The following equation is then obtained:

$$I_{pv} = I_{ph} - (I_{d2} + I_{d2}) - I_{Rsh} \quad (16)$$

With: I_{ph} and I_{Rsh} maintaining the same expressions as above Equation 2.

For the recombination currents, we have:

$$I_{d1} = I_{01}\left[\exp\left(\frac{q.(V_{pv} + R_s.I_{pv})}{A.n_s.k.T_j}\right) - 1\right] \quad (17)$$

$$I_{d2} = I_{02}\left[\exp\left(\frac{q.(V_{pv} + R_s.I_{pv})}{2.A.n_s.k.T_j}\right) - 1\right] \quad (18)$$

The saturation currents are written as:

$$I_{01} = P_4.T_j^3.\exp\left(\frac{-E_g}{k.T_j}\right) \quad (19)$$

$$I_{02} = P_5.T_j^3.\exp\left(\frac{-E_g}{2.k.T_j}\right) \quad (20)$$

With n_s is the number of cells in branched series, E_g represent the gap energy

The final equation of the model is thereby written as:

$$I_{pv} = P_1.E.\left[1 + P_2.(E - E_{ref}) + P_3.(T_j - T_{ref})\right] - \frac{(V_{pv} + R_s.I_{pv})}{R_{sh}} - P_{04}.T_j^3.\exp\left(\frac{-E_g}{k.T_j}\right).\left[\exp\left(q.\frac{V_{pv} + R_s.I_{pv}}{A.n_s.k.T_j}\right) - 1\right] \quad (21)$$
$$- P_{14}.T_j^3.\exp\left(\frac{-E_g}{2.k.T_j}\right).\left[\exp\left(q.\frac{V_{pv} + R_s.I_{pv}}{2.A.n_s.k.T_j}\right) - 1\right]$$

Figure 4 shows the current/voltage characteristics obtained using the three mathematic models compared with the experimental values corresponding to a 110 Wc Siemens panel (Table.1)

Table.1: Parameter of the PV panel SIEMENS SM110-24

Parameters	Values
P_{PV}	110W
I_{mpp}	3.15A
V_{mpp}	35V
I_{sc}	3.45A
V_{oc}	43.5V
α_{sc}	1.4mA/°C
β_{oc}	-152mV/°C
P_{mpp}	110W

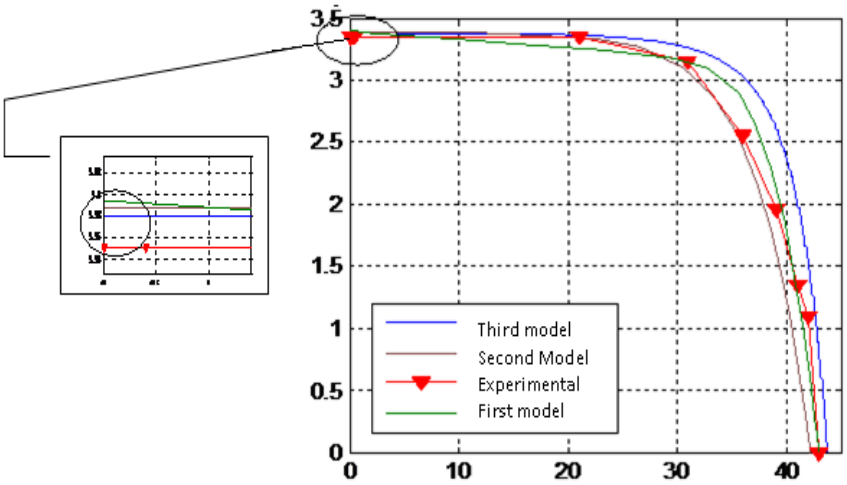

Fig.4. PV current versus PV voltage

2.2. Permanent-Magnet DC Motor (PMSM)

Due to absence of the field current and field winding, permanent magnet machines exhibit high efficiency in operation, simple and robust structure in construction and high power to weight ratio.

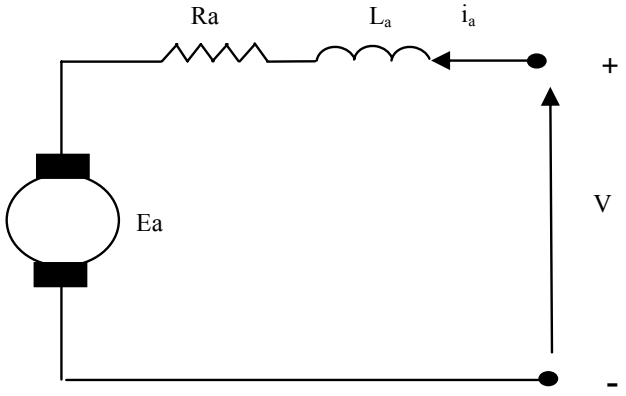

Fig.5. Equivalent circuit of PMSM

The motor produces, when it turning, a back emf E_A proportional to the angular speed

$$E_a = K.\omega \tag{22}$$

Where K is a constant

The DC voltage equation is:

$$V = R_a.I_a + K.\omega \tag{23}$$

The dynamical model can be written d as:

$$L_a \frac{di_a}{dt} = V_T - R_a i_a - K_m \omega \tag{24}$$

$$J\frac{d\omega}{dt} = K_m i_a - T_L \tag{25}$$

2.3. Controller

The controller used is a linear current booster (LCB). The MPPT maintains the input voltage and current of the LCB at the maximum power point of the photovoltaic module. As shown in (Fig.6), the power produced at the MPPis low-current and high voltage which is the opposite of those required by the pump motor. The LCB converts into high-current and low voltage which satisfies the pump motor characterirtics.

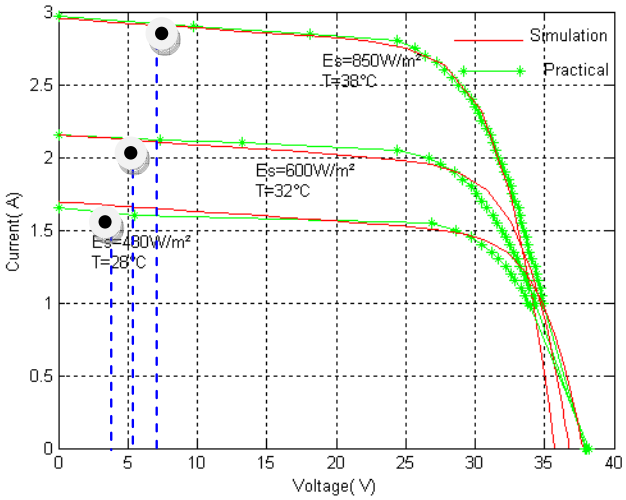

Fig.6. Photovoltaic I_{pv}-V_{pv} curves with DC motor I-V curve

2.4. Centrifugal pump model

In the centrifugal pump, the rotation of an impeller forces water into the pipe. The water velocity and pressure depend on the available mechanical power at the rotating impeller and the total head. A centrifugal pump commonly requires a single quadrant drive. Many research papers dealt with PV pumping systems modeling [6] has investigated a method to determine a PV pumping system performance by representing the water flow rate and efficiency of the system as function of supply frequency and pumping head. Ref [7] has used sets of differential equations to predict the behavior of a PV water pumping system depending on the level of solar global irradiance incident on the PV array. The characteristics have been represented by current, voltage, head (I, V, h) and water flow, current, head (Q, I, h) relationships [6]. The precedent models do not give the water flow output directly as a function of the electrical power input to the motor - pump subsystem. The actual model relates directly the pumped water flow output Q to the motor-pump subsystem electric power input P.

We use the model expresses the water flow output (Q) directly as a function of the electrical power input (P) to the motor-pump, for different total heads. The experimental data has been collected for several pumps by using the test bench. The collected data consists of measuring the water flow Q for different values of the electrical power input P and total head h. On the basis of these experiments, a model is elaborated by the use of the least-squares method to the set of measurements data.

A polynomial fit of the third order expresses the relationship between the flow rate and power input, as described by the following equation [6, 7]:

$$Q(h,P) = a(h)\,P^3 + b(h)\,P^2 + c(h)\,P + d(h) \tag{26}$$

where P is the electrical power input of the motor-pump, h is the total head and a(h), b(h), c(h), d(h) are the coefficients corresponding to the working total head [8].

$$a(h) = a_0 + a_1h^1 + a_2h^2 + a_3h^3 \tag{27}$$
$$b(h) = b_0 + b_1h^1 + b_2h^2 + b_3h^3 \tag{28}$$
$$c(h) = c_0 + c_1h^1 + c_2h^2 + c_3h^3 \tag{29}$$
$$d(h) = d_0 + d_1h^1 + d_2h^2 + d_3h^3 \tag{30}$$

With: a_i, b_i,, c_i and d_i constants which depend on the type of sub-solar pumping system.

The calculation of the instantaneous flow in terms of power is calculated using Newton-Raphson method. Thus at the k^{th} iteration, the flow Q is given by the following equation [7]:

For d – Pa (Q)> 0:

$$Q_k = Q_{k-1} - \frac{F(Q_{k-1})}{F'(Q_{k-1})} \tag{31}$$

With:

$$F(Q_{k-1}) = aQ^3_{k-1} + bQ^2_{k-1} + cQ_{k-1} + d - P_a(Q_{k-1}) \tag{32}$$

Where: $F'(Q_{k-1})$ is the derivative of the function $F(Q_{k-1})$

3. Photovoltaic pumping system efficiency

The PV array efficiency Eff_{PV} is defined as the ratio between the operating electric power and the incident power radiation on the tilted surface of a Photovoltaic module:

$$Eff_{pv} = \frac{P_{pv}}{E_s.S_{pv}.N_s.N_p} \tag{33}$$

Where P_{pv} is the operating electric power of the system (W), E_s is the global irradiance on the PV array (W/m^2), S_{pv} is the area of one module [m^2], Ns is the number of the module in series and N_p is the number of the modules in parallel in the PV array.

The pumping subsystem efficiency Eff_{pump} is defined as the ratio between the hydraulic power and the operating electrical power of the subsystem. The hydraulic power depends on the water flow rate and the total head. The equation of pumping subsystem efficiency Eff_{pump} is given as follows:

$$Eff_{pump} = \frac{\rho.g.Q.H}{3600.P_{pv}} \tag{34}$$

Where: ρ is the density of water, g is the acceleration due to gravity and 3600 is the number of second per hour, Q is the water flow rate (m^3/h), H is the total head (m).

The total efficiency of the PV pumping system is defined as the product of the efficiencies of thePV array and thepumping subsystem:

$$Eff_{total} = Eff_{pv}.Eff_{pump} \quad (35)$$

4. Experimental bench

The experimental bench is installed in the Laboratory LTII of the University of Bejaia. Figure 7 shows the experimental curves of the insolation and temperatures measured in the site and used in the experience to produce PV power and water flow rate.

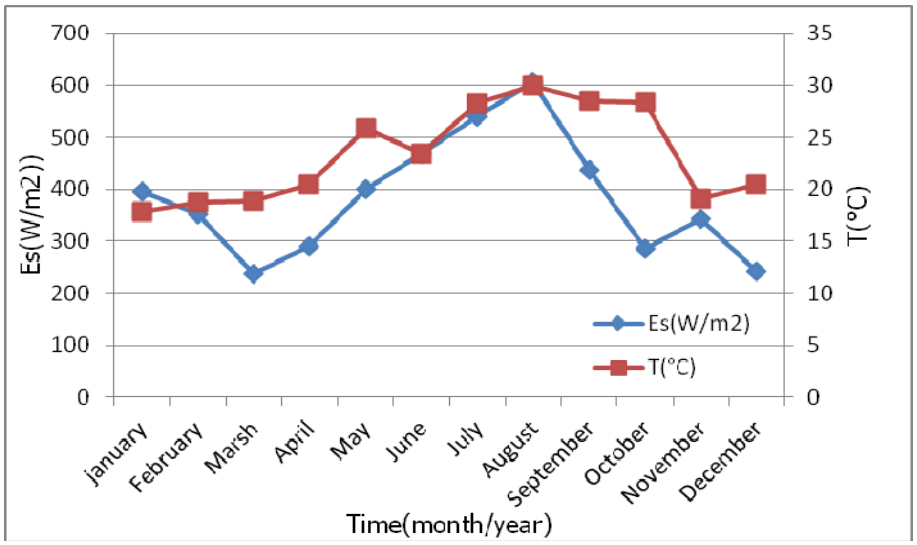

Fig.7.Experimental curves of the insolation and cell temperatures during a year at Bejaia

The main components of the experimental bench consist of mono-crystalline PV Siemens SM110-24 module with a peak power of 110Wp, a SHURFLO 9325 24V submersible pump a boost LCB, and a water tank. A motor operated valve is used to set the water head between 5, 9 and 13 m with flow rates ranging between 0 and 0.15 m^3 per hour.

Table.2: Parameter of the SHURFLO 9325 24V pump

Parameters	Values
Voltage rated	24 V DC
Maximum current	4.1A
Rated Power	120 W
Maximum submersion	30 m
Maximum lift	70 m

We make an application in a day of June 2012. Using the experimental bench, the performances of the pump is obtained for the peak power of the PV array (110 Wc) and

several levels of the total dynamic head (5, 9 and 13 m) and for different volumes of water (0.05, 0.15 and 0.15 m^3).

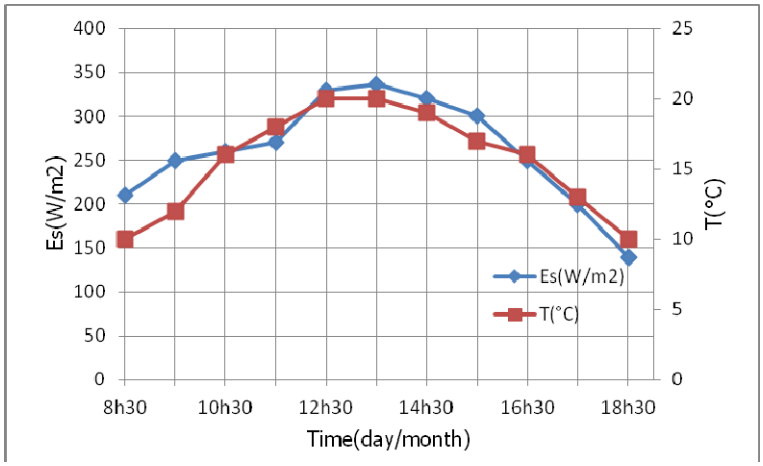

Fig.8. Insolation and cell temperature during a day

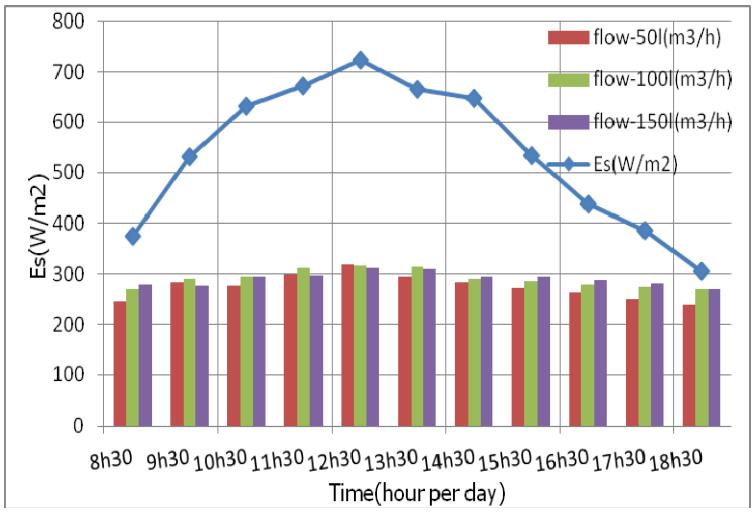

Fig.9. Insolation and water flow for different volume water at dynamic head of 13m

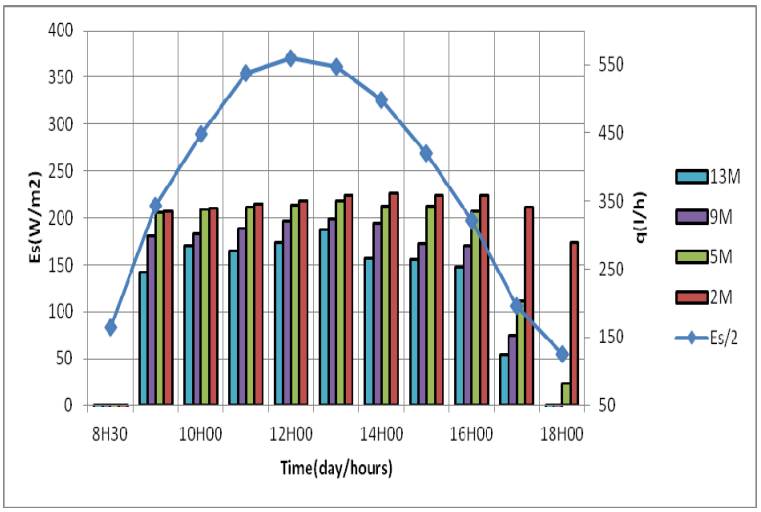

Fig.10. Flow variation for different dynamic head level during a day for V=0.15 m^3

Validation of the presented motor-pump subsystem model is performed at different head (2, 5, 9 and 13 m) and input power (Fig.9). Figure10 shows the average daily efficiencies for a head levelof 13m and a water volume of 0.15m^3. The maximal efficiency of pumping system is about 34 % and the total efficiency system is very low because the PV power is low and the application is made on defavorable day of insolation in december.

5. Conclusion

In this work, we have tested the operation of pumping systems destined to supply drinking water. The performances are compared in terms of total height and geographical site of Bejaia (Algeria).

The results show that the performance of the photovoltaic pumping system depends deeply on the pumping total head and the peak power of the photovoltaic array. We can conclude that the prototype system can be extended to a more powerful system.

References

[1] S. Lalouni, D. Rekioua, T. Rekioua, E. Matagne Fuzzy logic control of stand-alone photovoltaic system with battery storage ,Journal: of power sources, vol. 193, no. 2, pp. 899-907, 2009.
[2] F. Chekired, C. Larbes, D. Rekioua, F. Haddadi, Implementation of a MPPT fuzzy controller for photovoltaic systems on FPGA circuit, Journal: Energy Procedia , vol. 6, pp. 541-549, 2011.
[3] C. Franx, A New Approach to Using Solar Pump Systems Submersible Motors, Proceedings of the 2nd Photovoltaic Solar Energy Conference, pp. 1038 - 1045, 1979.
[4] D.S.H. Chan, J. R. Philips and J.C.H. Phang, A Comparative Study of Extraction Methods for Solar Cell Model Parameters, Solid State Electronics, Vol. 29, No. 3, pp. 329-337, 1986.
[5] L. Keating, D. Mayer, S. McCarthy and GT Wrixon, Concerted Action on Computer Modeling and Simulation, Proceedings of the 10th European Photovoltaic Solar Energy Conference, Lisbon, Portugal, pp. 1259 - 1265, 1991.
[6] A. Hamidat, Simulation of Photovoltaic Pumping Systems Intended for Food and Drinking Water and Irrigation for Small, PhD thesis, University Abou Bakr Belkaid, Tlemcen, 2004.
[7] S.Ould Amrouche, D.Rekioua, A.Hamidat, Modeling photovoltaic water pumping systems and evaluation of their CO2 emissions mitigation potential, Applied Energy, vol. 87, no. 11, pp. 3451-3459, 2010.
[8] D. Rekioua and E. Ernest, Optimization of Photovoltaic Power System: Modelization, Ed.Springer; (2012).